

Enabling High-Resolution Photon-Counting Measurements Near Cloud Edges

Grant J. Kirchhoff^(a), Matthew Hayman^(b), Willem J. Marais^(c), Jeffrey P. Thayer^(a), and Rory A. Barton-Grimley^(d)

^(a) University of Colorado Boulder, Aerospace Engineering Sciences Department
Boulder, CO, USA 80303

^(b) NSF National Center for Atmospheric Research, Earth Observing Lab
Boulder, CO, USA 80303

^(c) University of Wisconsin Madison, Space Science & Engineering Center
Madison, WI, USA 53706

^(d) NASA Langley Research Center
Hampton, VA, USA 23681
grant.kirchhoff@colorado.edu

Abstract: Single-photon avalanche diodes exhibit a nonlinear bias known as *deadtime*, in which high-density backscatter signals can saturate the detector. This results in missed counts and measurements that are biased low, thus limiting the detector’s dynamic range. Unfortunately, traditional *deadtime* correction (via post-processing) is limited only to applications where the scene of interest is uniform over the sampling bin. This means it fails to accurately estimate dynamic or heterogeneous scenes that exhibit high backscatter, posing a significant challenge. This presentation introduces a novel *deadtime*-correction technique that overcomes these limitations, enabling high-resolution measurements at high (and low) fluxes. We leverage this new capability in combination with an ultra-high-resolution acquisition system (< 1 cm) to generate high-resolution measurements of clouds. This will be demonstrated using simulations and measurements.

1. Introduction

Photon-counting detectors struggle to produce linear measurements in high-flux regimes because of a characteristic known as *deadtime*. For single-photon avalanche diode (SPAD) detectors, *deadtime* manifests as a reset period immediately following a detection event where the detector is inactive (or “dead”). In high-density backscatter conditions, this results in missed counts, which causes measurements to be biased low. Traditionally, this nonlinear bias has been corrected by the Müller Correction (popularized by Donovan et al.) [1, 2] in post-processing:

$$\rho = \frac{R}{1 - R\tau} \quad (1)$$

where ρ is the unbiased mean photon count rate, R is the measured count rate, and τ is the *deadtime* interval. The (often overlooked) approximation that is made when applying for the Müller Correction is that the measured count rate (calculated as $R = \langle N \rangle / \Delta t$, where $\langle N \rangle$ is the average number of photon counts in

a bin and Δt is the bin-accumulation interval) represents an independent measurement of a uniform flux over the bin duration. This can be organized into two related approximations that will be called the “Müller Approximations”:

1. **Approximation #1:** The photon flux during a bin interval Δt is approximately constant.
2. **Approximation #2:** Each observation bin is unaffected by observations in other bins. This is generally valid when Approximation #1 holds *and* the bin time Δt is much larger than the *deadtime* τ , i.e., $\Delta t \gg \tau$.

Approximation #1 is violated when using a sampling interval that is too coarse for the flux variability. The consequences of violating Approximation #1 are seen in Fig. 1 (top), showing two unique measurements of a single, narrow Gaussian target (with $\sigma = 10\tau$ and $\tau = 25$ ns) acquired at high ($\Delta t_f = \tau$) and low resolution (where $\Delta t_c = 2 \mu s$). In Fig. 1 (bottom), measurements of the same target at

low resolution are processed while increasing the target's amplitude. The results show that applying the Müller Correction to an undersampled target (low resolution) with fine-scale structure produces inaccurate estimates whose errors increase as a function of peak flux.

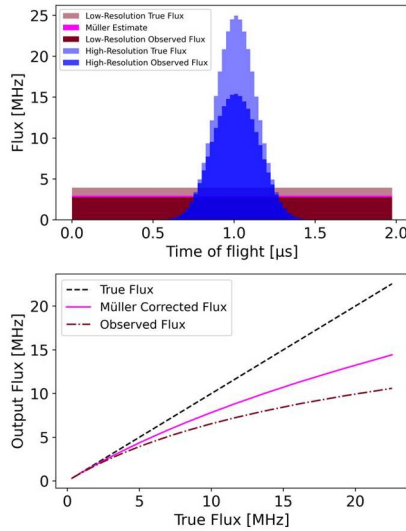


Figure 1. Müller Correction inaccuracy when violating Approximation #1.

An intuitive approach to overcome this issue would be to reduce the sample bin size to avoid undersampling the scene; however, for variability that occurs on range scales close to the range-equivalent deadtime length (e.g., 4.5 meters for 30 ns deadtime), using a resolution that matches this variability results in the violation of Approximation #2. This contradiction between the two requirements shows that a different approach is needed for deadtime correction when measuring variable high-flux targets.

2. Deadtime Model and Correction

We developed a new deadtime-correction technique (DCT) that leverages a deadtime noise model to generate a maximum-likelihood estimator to correct deadtime bias. The benefit of the DCT is that no assumptions or restrictions are placed on the scene type or acquisition. As a result, the DCT enables high-resolution measurements of high- and low-flux targets. Using the histogram model (the common acquisition approach in photon counting), the loss function \mathcal{L}_D used for the maximum-likelihood estimator is given by

$$\mathcal{L}_D(\rho(t); \mathbf{t}) = \sum_{m=1}^M N \rho_m Z_m \Delta t - Y_m \ln \rho_m \quad (2)$$

where t represents the 1D range-equivalent time axis, \mathbf{t} is the set of photon detection times relative to each laser shot, M is the total number of sampling bins, N is the number of laser shots, Y_m is the standard photon-count histogram, Z_m is a histogram that tracks the average impact of deadtime from preceding bins and $\rho_m \triangleq \rho(t_m)$ under the zero-order hold assumption for sampling. For a given measurement, the optimal count-rate profile $\tilde{\rho}(t)$ would be obtained via parametric fitting by optimizing over polynomial complexity J , a background term b , and coefficients $\mathbf{c} = \{c_j\}_{j=1}^J$:

$$\tilde{\rho}(t) = \underset{\mathbf{c}, b}{\operatorname{argmin}} \mathcal{L}_D(\rho(\mathbf{c}, b, t); \mathbf{t}) \quad (3)$$

The DCT was then tested by simulating a high-flux, narrow Gaussian target (i.e., $\text{FWHM} \ll \tau$, in violation of Approximation #2 for the Müller Correction). The DCT performed remarkably well at recovering the actual flux profile, shown in Fig. 2. The Poisson fit (assuming negligible deadtime bias, $\tau = 0$) results are included for comparison since a common data-processing approach assumes negligible deadtime bias in low-flux regions. Recall that the Müller Correction is inaccurate when applied to a narrow target like this because of the violation of Requirements #1 and #2 for this scene and acquisition combination. The deadtime fit also performed remarkably well at low flux (< 1 MHz), thus demonstrating its flexibility by enabling high- and low-flux measurements at ultra-high resolutions (i.e., sub-meter), previously infeasible when using the Müller Correction.

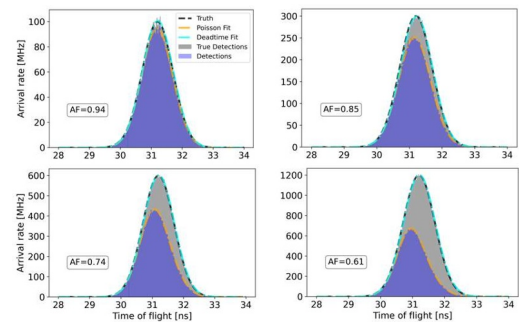


Figure 2. Deadtime fit results for a simulated narrow profile.

The accuracy of the correction technique has also been demonstrated experimentally in work currently in preparation for publication, but for brevity, the results will not be discussed in this document.

3. High-Resolution Cloud Measurements

The deadtime-correction technique enables high-resolution measurements of high-flux targets, thus simultaneously enhancing the precision and dynamic range of photon-counting detection. It would be promising to leverage this new capability to investigate atmospheric targets historically limited by dynamic range and precision issues. Ultra-high resolutions (sub-centimeter) are now achievable using time-correlated single-photon counting (TCSPC) acquisition. Cloud edges are an example of a variable and dynamic target inadequately measured. A backscatter-density curtain plot showing this type of ground-based measurement using the CU Boulder Backscatter Lidar (CUBL) is shown in Fig. 3.

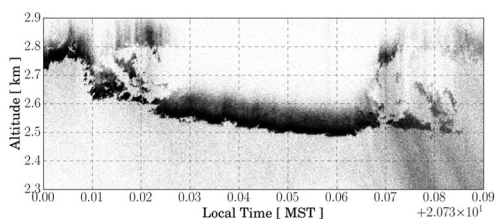


Figure 3. Ultra-high-resolution cloud-base measurement (image source [5]).

The measurement was acquired using TCSPC at ultra-high-range resolution (4 mm). The dense backscatter signal spanning 2.5 and 2.9 km discriminates the cloud edge. Still, interesting fine-scale features exist immediately below the cloud (including what is possibly virga near local time 20.81), thus highlighting the fine-scale variability within and near cloud bases. Modern ceilometer cloud-base measurements are limited to 10-m vertical resolution [6], so many fine-scale features would be missed. The measurement in Fig. 3 displays raw photon-count density and was uncorrected for deadtime, so there exists potential to pair TCSPC and the DCT to recover these high-flux, fine-scale features with unprecedented precision accurately. This new capability will enable the definition of a benchmark for what types of resolutions are now feasible for atmospheric lidars. This

benchmark will be valuable to atmospheric science communities (e.g., cloud physics, meteorology) where resolution limits for cloud-base and -top observations must be better defined.

To test this further, an attenuated-backscatter retrieval was simulated using CUBL's parameters, including a low-power laser (1.5 μJ) and moderate-aperture telescope (203 mm), as well as standard scattering parameters for low-level liquid water clouds ($\beta = 10^{-3} \text{ m}^{-1} \text{ sr}^{-1}$, $\alpha = 20\beta \text{ m}^{-1}$). The simulation results for a low-level, static cloud ground-based measurement are shown in Fig. 4. At low altitude, the overlap function becomes unity at 550 m, in which the Rayleigh signal return is observable at altitudes leading up to the cloud base at 1 km. The cloud extends from 1 – 2 km, where it is apparent that deadtime bias results in many missed counts at and above the cloud's bottom edge (integrated over 10^3 laser shots, or 68 ms of accumulation).

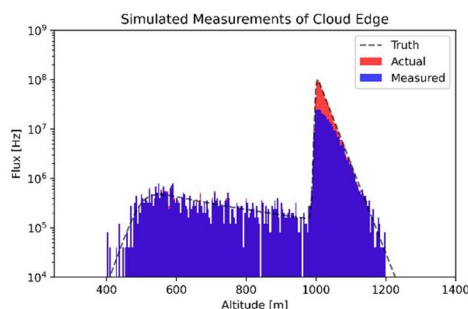


Figure 4. Simulated cloud-edge measurements using CUBL.

Even though extinction attenuates the signal rapidly within the cloud, the actual signal in the first 50 - 100 m of the cloud is at (1) detectable signals that are large enough to minimize averaging over fine-scale structure and (2) the measured signal should be correctable using the deadtime correction technique, and sufficiently noise suppressed to maintain ultra-high resolution. Deadtime bias becomes nonnegligible for instantaneous fluxes greater than 10 MHz, and this simulation demonstrates that these types of fluxes are encountered near the cloud edge by a low-power backscatter-lidar system. There are ongoing developments to apply the DCT to these simulated profiles and quantify its benefit across a large parameter space i.e., varying integration periods, resolution, temporal variability. Cloud edges are inherently heterogeneous in range and

dynamic in time, so understanding how to measure a time-varying target like a cloud accurately is critical and, as mentioned previously, will ultimately inform the benchmark for what types of vertical and horizontal resolutions are possible using TCSPC and the deadtime-correction technique in combination.

Ultimately, the hypothesis will be tested on actual cloud measurements. A low-power attenuated-backscatter lidar system, with the specifications included in Tab. 1, is currently being assembled at the University of Colorado Boulder.

Table 1. Instrument Specifications

Laser Transmitter	$\lambda = 532.18 \text{ nm}$ Frequency = 14.3 kHz Energy = 1.5 μJ FWHM < 700 ps
SPAD Detector	Pulse width = 17.1 ns Deadtime = 29.1 ns
Acquisition	Bin width = 25 ps Deadtime < 25 ns

In this system, we have ensured that the detector deadtime is longer than the acquisition deadtime to ascertain that the deadtime bias only comes from the detector, which is necessary for the deadtime-correction technique. With this system, the edges of low-level, liquid-water clouds will be measured and processed at ultra-high resolution using the DCT. This work is in development and will be updated before the conference.

4. Conclusions

When processing photon counting data in atmospheric lidar, the traditional approach to deadtime correction (or Müller Correction) is limited to measuring uniform scenes sampled over very coarse grids. To overcome these limitations, we presented a novel deadtime-correction technique (DCT) that more accurately models deadtime behavior in SPAD detectors to generate a maximum-likelihood estimator to correct for deadtime bias. The accuracy of the DCT has been demonstrated on high-resolution simulated and experimental measurements of targets with fine-scale variability. This showed that the DCT could enable measurements of high-flux atmospheric

targets with high spatial and temporal variability.

Ultra-high-resolution cloud-edge measurements were also obtained using a low-power attenuated-backscatter lidar system, demonstrating the incredibly complex structure (< 1 m) near the cloud edge that is currently missed by modern ceilometer cloud-measurement resolutions (10 m). We propose to use ultra-high-resolution acquisition (TCSPC) in combination with the DCT to accurately estimate high-flux, high-variability atmospheric targets (such as cloud edges) and thus explicitly quantify flux and resolution limits for atmospheric lidars when using this approach. This poorly defined benchmark will help inform atmospheric science communities requiring high-resolution cloud-edge observations. Simulation demonstrated that cloud penetration is severely limited by deadtime for at least 100 m (before extinction dominates the backscatter-signal strength) and that the expected flux levels near the cloud edge should be correctable using the DCT. Ongoing work includes applying the deadtime-correction technique to the simulated retrievals and building a backscatter-lidar system to execute these tests on measurements of cloud edges, which will be updated for the conference presentation.

5. References

- [1] D. Donovan, J. Whiteway and A. Carswell, "Correction for nonlinear photon-counting effects in lidar systems," *Applied Optics*, p. 6742–6753, 1992.
- [2] J. W. Müller, "Dead-time Problems," *Nuclear Instrument Methods*, vol. 112, pp. 47-57, 1973.
- [3] V. R. Morris, "Ceilometer Instrument Handbook," DOE Office of Science Atmospheric Radiation Measurement (ARM) User Facility, Washington D.C., 2016.
- [4] R. A. Barton-Grimley, *Single Photon Counting Lidar Techniques and Instrumentation for Geoscience Applications*, University of Colorado Boulder: Ph.D. Thesis, 2019.